Mol Breeding (2023) 43:57
https://doi.org/10.1007/s11032-023-01404-1

The TabHLH094–TaMYC8 complex mediates the cadmium response in wheat

Xuye Du · Lihe Fang · Jiaxing Li · Tianjiao Chen · Zai Cheng · Bin Zhu · Lei Gu · Hongcheng Wang

Received: 17 January 2023 / Accepted: 8 July 2023 / Published online: 12 July 2023

Abstract In wheat, TaMYC8 is a negative regulator of cadmium (Cd)-responsive ethylene signaling. In this study, we functionally characterized TabHLH094, a basic helix–loop–helix (bHLH) transcription factor (TF) that inhibits the transcriptional activity of TaMYC8. The TabHLH094 protein was found in the nucleus of tobacco epidermal cells and exhibited transcriptional activation activity. Real-time quantitative PCR (RT–qPCR) indicated that *TabHLH094* exhibited root-specific, Cd-responsive expression in wheat seedlings. Overexpression of *TabHLH094* enhanced the tolerance of wheat seedlings to Cd exposure. The protein–protein interaction between TabHLH094 and TaMYC8 was verified by glutathione S-transferase (GST) pulldown, coimmunoprecipitation (Co–IP), yeast two-hybrid (Y2H), and bimolecular fluorescence complementation (BiFC) analyses. TabHLH094 was found to reduce the ability of TaMYC8 to bind to the TaERF6 promoter. Furthermore, TabHLH094 could also reduce aminocyclopropanecarboxylate oxidase (ACO) and ACC synthase (ACS) activities, both of which are necessary for ethylene biosynthesis. Taken together, these results indicate that TabHLH094 mediates Cd tolerance by regulating the transcriptional activity of TaMYC8 and decreasing ethylene production.

Keywords Wheat · *TabHLH094* · *TaMYC8* · Complex · Cadmium

Introduction

One highly significant threat to global soil quality is heavy metal contamination. Although heavy metals are present naturally in many soils, human activities are responsible for increasing their concentration in many contexts (Ma et al. 2020a). In particular, industrial activities, fossil fuel combustion, inadequate sewage sludge treatment, and the overuse of chemical fertilizers and pesticides have been linked to increased heavy metal contamination (Leškovï et al. 2020). Because plants are capable of bioaccumulating heavy metals, these pollutants can enter the food web and endanger both animal and human health (Zhao et al. 2018).

Exposure to the toxic and nonessential heavy metal cadmium (Cd) is severely harmful to living cells (Brunetti et al. 2015), even at miniscule concentrations (Elobeid et al. 2012). In plants, Cd exposure can lead to destruction of the photosynthetic system, a reduction in leaf photosynthetic

Xuye Du and Lihe Fang contributed equally to this work.

Supplementary Information The online version contains supplementary material available at https://doi.org/10.1007/s11032-023-01404-1.

X. Du · L. Fang · J. Li · T. Chen · Z. Cheng · B. Zhu · L. Gu · H. Wang (✉)
School of Life Sciences, Guizhou Normal University, Guiyang, Guizhou Province, China
e-mail: besthongcheng@163.com

capacity, inhibition of root elongation, and even death (Ma et al. 2020b). Because Cd contamination of agricultural soils poses such a high risk to plants, developing Cd stress-resistant crop cultivars is critical for food safety and security.

In plants, the extensive basic helix–loop–helix (bHLH) transcription factor (TF) superfamily regulates an array of physiological operations (Mao et al. 2017), including the physiological and biochemical responses to environmental stress exposure (Xu et al. 2017). For instance, the transgenic expression of maize-derived *ZmbHLH124* results in significantly increased tolerance to water scarcity (Wei et al. 2021). Salt-inducible *OsbHLH035* is expressed primarily in germinated rice seeds and seedlings (Chen et al. 2018). In *Arabidopsis*, *AtbHLH39* overexpression confers enhanced tolerance to Cd exposure (Wu et al. 2012). Recently, we found that the wheat-derived bHLH-type TF *TaMYC8* negatively regulates the Cd stress response (Wang et al. 2022a, b).

Mounting evidence suggests that interactions between proteins may be crucial for the regulation of gene expression. Specifically, many TFs interact with other TFs to form homo- and heterodimeric complexes. For example, jasmonic acid-mediated anthocyanin accumulation is regulated by the WD–Repeat/bHLH/MYB complex in *Arabidopsis* (Qi et al. 2011). In *Brassica napus*, resistance to *Sclerotinia* infection is regulated by the interaction between BnWRKY15 and BnWRKY33 (Liu et al. 2018). In *Medicago truncatula*, nitrogenase activity is maintained during drought stress by the interaction between MtCAS31 and MtLb120–1 (Li et al. 2018).

Here, we sought to functionally characterize the wheat-derived bHLH TF *TabHLH094* in regulating the uptake of and tolerance to Cd. We found that overexpression of *TabHLH094* resulted in decreased root-to-shoot translocation of Cd. Additionally, we found that TabHLH094 interacts with the bHLH-type TF TaMYC8, thereby inhibiting the ability of this TF to interact with the promoter of *TaERF6*. The resultant induction of *TaERF6* expression affected ethylene biosynthesis and conferred tolerance to Cd exposure in wheat. The results of this study help clarify the mechanism by which bHLH TFs regulate the wheat Cd stress response.

Materials and methods

Plant materials

We germinated seeds of "Fielder" wheat (*Triticum aestivum* L.) on sterile filter paper. After 5 days, seedlings exhibiting uniform growth were transplanted into sand. Seedlings were watered daily with half-strength Hoagland medium. Three-leaf-stage wheat seedlings were watered with Hoagland medium mixed with either 0 (control) or 2 mM (experimental) $CdCl_2$ for either 3 h or 5 days, depending on the experiment.

Soil pot experiments were carried out at the greenhouse of Guizhou Normal University, Guiyang, China. The potting soil consisted of clay and humus and was prepared at a ratio of 1:1. The treatment group was supplemented with Cd at a dose of 5 mg/kg. Plant seeds were first sterilized and sown in ddH_2O to germinate and then transferred to soil. After complete maturation, the seeds were harvested for further analysis.

TabHLH094 expression

Total RNA was sampled from both the aerial and root tissues of wheat seedlings and reverse-transcribed into cDNA using kits purchased from CwBio (Beijing, China). *Taβ–actin* was used as the internal reference. Real-time quantitative PCR (RT–qPCR) was accomplished utilizing SYBR Green Super Mix (CwBio, Beijing, China) with a QuantStudio 3 RT–PCR System (Thermo Fisher Scientific, MA, USA).

Determination of subcellular localization

The *TabHLH094* coding DNA sequence (CDS) was inserted into the pBI121–GFP vector after digestion with *EcoR* V. Subsequently, the *35S*::*TabHLH094*–GFP construct was introduced into *Agrobacterium tumefaciens* "GV3101," and these cells were used to transform tobacco epidermal cells. Detection of TabHLH094–GFP fluorescence was performed using an FV500 confocal laser-scanning microscope (Olympus, Tokyo, Japan).

Transcriptional activation assay

The *TabHLH094* CDS was digested with *EcoR* V and *BamH* I and integrated into the pGBKT7 vector. The recombinant construct was then introduced into *Saccharomyces cerevisiae* "AH109." The method of Song et al. (2020) was used for all transcriptional activation assays.

Vector construction and genetic transformation

To produce a plasmid for *TabHLH094* overexpression lines, the *TabHLH094* CDS was cloned into the pCambia1300 vector (Supplementary Fig. S1). Immature "Fielder" wheat embryos were transformed through *Agrobacterium*-mediated gene transfer (Jin et al. 2021). Three independent T2 generation *TabHLH094* overexpression lines were selected for further analysis.

Cd content analysis

Leadmium Green AM Dye (Thermo Fisher Scientific, MA, USA) was utilized to visualize Cd accumulation in root tissues. After exposing WT and transgenic wheat lines to 2 mM Cd for 5 days, the roots were washed with ddH_2O and subsequently soaked in Leadmium Green AM Dye (5 µL/mL) for 6 h. Fluorescence (480 nm) was detected with an FV500 confocal laser-scanning microscope (Olympus, Tokyo, Japan). Fluorescence intensity was quantified by measuring fluorescence pixel intensity with ImageJ software (Liu et al. 2018). To quantify the Cd concentration in root tissues, WT and transgenic wheat seedlings were exposed to 2 mM Cd for 5 days, after which the roots were collected and rinsed with ddH_2O and subsequently dried at 60 °C. The content of Cd in wheat tissues was quantified using inductively coupled plasma–mass spectrometry (ICP–MS) (Thermo Fisher Scientific, MA, USA).

Electrophoretic mobility shift assay (EMSA)

Utilizing our previously published method (Wang et al. 2022a, b), the 5′–GGCAAACTCACGTTC GTCCATTGCA–3′ sequence was labeled at the 3′ end with biotin as the hot probe. The *TaMYC8* and *TabHLH094* CDSs were cloned into the pET32a vector to produce the TaMYC8–His and TabHLH094–His fusion proteins, respectively. LightShift Chemiluminescent EMSA Kits (Thermo Fisher Scientific, MA, USA) were utilized for all EMSA experiments.

Yeast two-hybrid (Y2H) experiment

The Y2H experiment was performed utilizing the Matchmaker Gold Y2H System (Clontech, CA, USA) using the manufacturer's standard directions. Briefly, the TabHLH094 and TaMYC8 CDSs were cloned into the pGBKT7 and pGADT7 vectors, respectively. The recombinant constructs were then cotransformed into *Saccharomyces cerevisiae* "AH109."

Coimmunoprecipitation (Co–IP) experiment

The TabHLH094 and TaMYC8 open reading frames (ORFs) were inserted into the pTCK303–Flag and pCAMBIA2300–MYC binary vectors, respectively. To study the interaction between TabHLH094 and TaMYC8, both *35S*::*TabHLH094*–Flag and *35S*::*TaMYC8*–MYC were transiently coexpressed in tobacco leaves. Anti-Flag affinity gel (Abmart, Shanghai, China) was used to precipitate Flag-fused protein. Anti-MYC and anti-Flag antibodies (Abmart, Shanghai, China) were utilized for immunoblotting.

GST pulldown experiment

To study the interaction between TabHLH094 and TaMYC8, the TabHLH094–His and TaMYC8–GST fusion proteins were expressed in pET32a–TabHLH094 or pGEX–4 T–1–TaMYC8 construct-carrying *Escherichia coli* "BL21(DE3)." Purification of fusion proteins was performed with either a GST–Tag Protein Purification Kit (Beyotime, Shanghai, China) or a His–Tagged Protein Purification Kit (CwBio, Beijing, China). The pulldown assay was then performed using a GST pulldown kit (FitGene, Guangzhou, China).

Bimolecular fluorescence complementation (BiFC)

The TabHLH094 and TaMYC8 ORFs were inserted into the *EcoR* V-digested pXY106 vector and the *BamH* I-digested pXY104 vector to construct the TabHLH094–nYFP and TaMYC8–cYFP fusion proteins, respectively. The plasmid combinations were infiltrated into tobacco leaves using *A. tumefaciens*.

Yellow fluorescent protein (YFP) in tobacco leaves was visualized with an FV500 confocal laser-scanning microscope (Olympus, Tokyo, Japan).

Luciferase complementation imaging (LCI) experiment

The reporter construct was produced by inserting the *TaERF6* promoter into pGreenII 0800–LUC. The effectors were constructed by inserting the ORFs of *TabHLH094* and *TaMYC8* into pGreenII 62–SK. Subsequently, four *A. tumefaciens* combinations were infiltrated into four distinct portions of the same individual tobacco leaves. After culturing the tobacco leaves for 36 h, each leaf was treated with 100 mM luciferin and kept for 5 min in darkness prior to luminescence detection. A NightOWL II LB 983 low-light cooled CCD imaging apparatus (Berthold Technologies, Bad Wildbad, Germany) was utilized to measure luciferase activity.

Aminocyclopropanecarboxylate oxidase (ACO) and ACC synthase (ACS) activities

To each sample of plant material (1 g), 10 μM pyrrolyl phosphate (PLP), 3% crosslinked polyvinylpyrrolidone (PVPP), 1 mM phenylmethylsulfonyl fluoride (PMSF), 0.1 M potassium phosphate buffer (pH 8.0), 1 mM acetylphenylenediamine tetraacetic acid (EDTA), and 4 mM dithiothreitol (DTT) were added. The mixture was centrifuged at 12,000 g and 4 °C for 15 min. A 500 μL sample of the supernatant was incubated in 1.5 mL of a mixture containing 10 μM PLP, 0.1 M potassium phosphate buffer (pH 8.0), and 250 μM s–adenosylmethionine (SAM). Incubation of the reaction mixture was carried out at 30 °C for 1 h, after which we added 700 μL of 0.1% $HgCl_2$ to arrest the reaction. The arrested reaction mixture was subsequently incubated for 10 min at 4 °C, after which 200 μL of a precooled NaOH solution saturated with 5% NaClO (NaClO:NaOH = 2:1, v/v) was added. The method of Zhang et al. (2018) was utilized for the measurement of ACO and ACS enzymatic activities.

Statistical analyses

All of the assays were performed under controlled environmental conditions utilizing three biological replicates. Statistically significant differences among treatments were analyzed with either Student's *t*-tests or one-way analysis of variance (ANOVA).

Primers

Each primer utilized in the present work can be found in Supplementary Table S1.

Results

TabHLH094 is positively regulated by Cd exposure

To determine the Cd responsiveness of *TabHLH094*, wheat seedlings were exposed to Cd, and the transcript level of *TabHLH094* was analyzed and compared to that of untreated (control) seedlings. Exposure to Cd resulted in a significant upregulation of *TabHLH094* expression in both roots and shoots (Fig. 1a), indicating that *TabHLH094* is involved in the reaction of wheat seedlings to Cd exposure.

TabHLH094 is located in the nucleus

The subcellular localization of the TabHLH094 protein was examined in tobacco epidermal cells. TabHLH094 is located in the nucleus (Fig. 1b), which is consistent with its TF functionality.

TabHLH094 overexpression increased tolerance to Cd exposure

To functionally characterize the *TabHLH094* gene, transgenic *TabHLH094*-overexpressing wheat plants were generated. Five independent transgenic lines were obtained and identified through PCR (Supplementary Fig. S2). RT–qPCR was further used to determine the expression of *TabHLH094* in different transgenic lines, and two lines with the highest expression (OE1 and OE2, Supplementary Fig. S3) were selected for the follow-up experiment. Both WT and transgenic wheat exhibited similar phenotypes under control conditions. However, under Cd treatment, WT wheat exhibited significantly weaker growth and shorter roots than transgenic wheat (Fig. 2a). Furthermore, under Cd conditions, the root and shoot dry weights of transgenic wheat were significantly

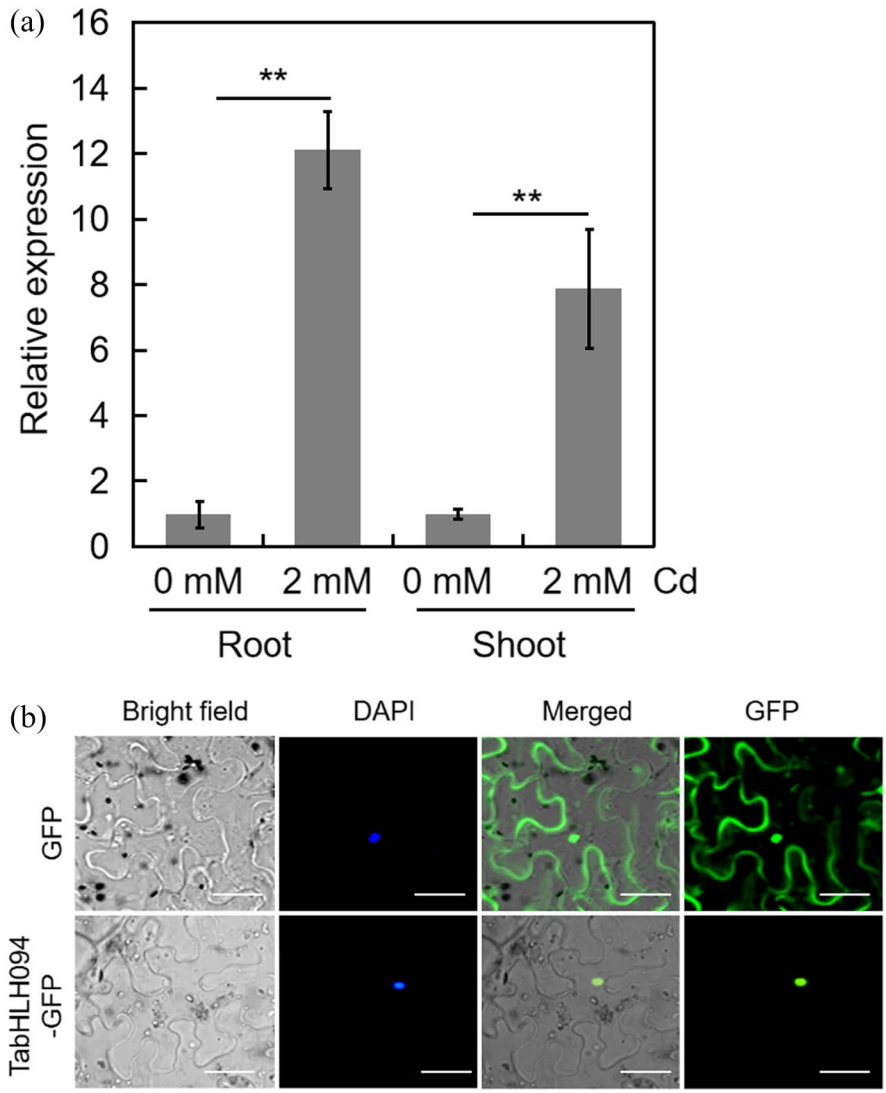

Fig. 1 Expression of *TabHLH094* and subcellular localization of TabHLH094. **a** *TabHLH094* expression in Cd-treated wheat, as determined by RT−qPCR. Each value is the mean ± SE ($n = 3$). Significant differences were analyzed by Student's *t*-test. $^{**}P < 0.01$. **b** Subcellular localization of TabHLH094:GFP in tobacco epidermal cells. Scale bars = 50 μm

higher than those of WT (Fig. 2b). Our results suggest that *TabHLH094* overexpression enhances plant tolerance to Cd exposure.

Overexpression of *TabHLH094* inhibits uptake of Cd

To visualize Cd accumulation in root tissue, wheat seedlings were exposed for 5 days to 2 mM Cd, after which the roots were soaked in Leadmium Green AM Dye for 6 h. Overall, WT wheat accumulated significantly more Cd in root tissues than transgenic wheat (Fig. 3a, b). ICP–MS was then used to quantify the content of Cd in the roots. Consistent with the fluorescence results, both the roots and shoots of WT wheat were found to contain a higher concentration of Cd than transgenic wheat (Fig. 3c). Furthermore, the average transfer coefficients of Cd in the WT and transgenic lines were 0.86 and 0.54, respectively. Our results suggest that *TabHLH094* overexpression reduces the uptake of Cd into root tissues and reduces the transport of Cd to shoots.

Overexpression of *TabHLH094* promotes growth and decreases the grain Cd content of wheat

The effect of *TabHLH094* overexpression on plant growth and grain Cd content in wheat under pot conditions was assessed. The growth of transgenic

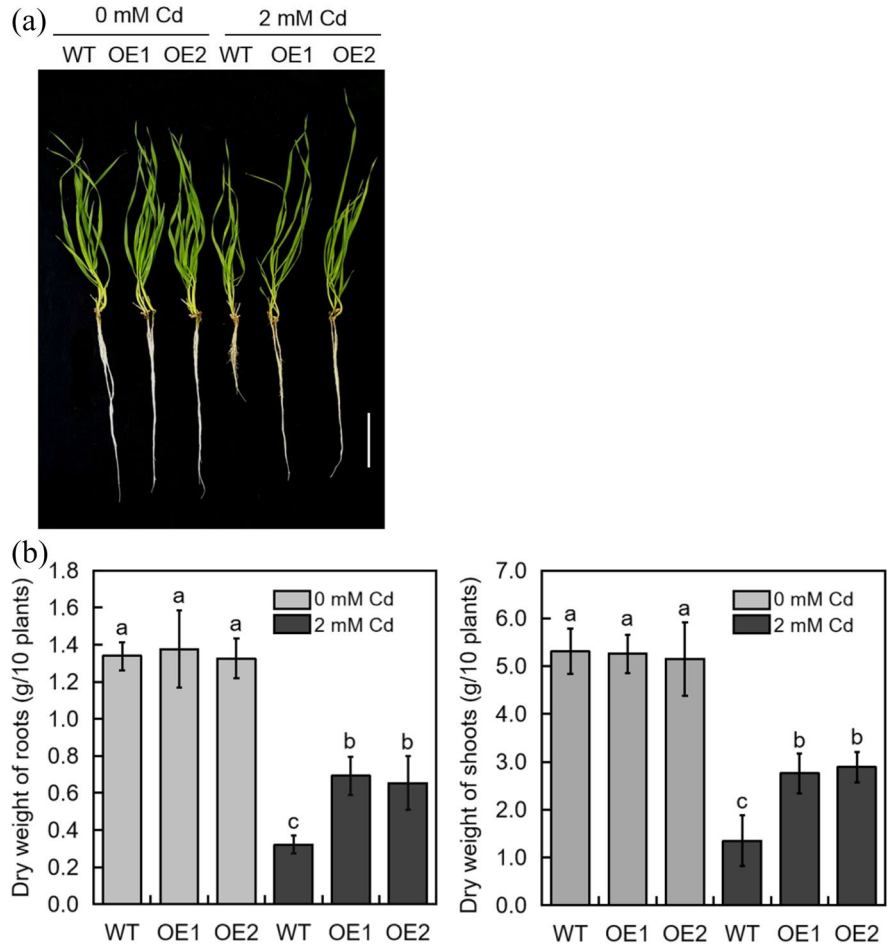

Fig. 2 *TabHLH094* positively regulates Cd tolerance in wheat. **a** Phenotypes of Cd-treated WT and transgenic wheat. Three-leaf-stage wheat seedlings were watered with Hoagland medium mixed with 2 mM (experimental) $CdCl_2$ for 5 days. Scale bar = 5 cm. **b** Dry weight of control and Cd-treated WT and transgenic wheat. Each value is the mean ± SE ($n = 3$). Different lowercase letters signify significant ($P < 0.05$) differences

plants under Cd stress treatment was better than that of WT plants (Fig. 4a), and the grain scales of transgenic wheat lines were significantly larger than those of the WT (Fig. 4b). Furthermore, the thousand-grain weight was measured, and Cd stress decreased the thousand-grain weight of WT plants compared with transgenic lines (Fig. 4c). Under Cd conditions, the average thousand-grain weight was 27.6 g for the WT lines and 34.7 g for the transgenic plants. We next analyzed the grain Cd content. As shown in Fig. 4d, the Cd content in the WT was significantly higher than that in the transgenic lines. The average Cd content in the WT wheat grains was 0.32 mg/kg, while in the transgenic plant grains, the average Cd content was 0.18 mg/kg. Thus, overexpression of *TabHLH094* promoted the growth of transgenic wheat under Cd stress and decreased Cd accumulation in wheat grains.

TabHLH094 interacts with TaMYC8

RNA was extracted from the leaves of Cd-exposed wheat and utilized to construct a cDNA library. TabHLH094 was used as bait in a Y2H screening assay to identify potential protein interaction partners. Sequence analysis of candidate proteins indicated that the bHLH-type TF TaMYC8 can directly interact with TabHLH094. We validated the physical interaction between TabHLH094 and TaMYC8 using a Y2H assay. We found that cells coexpressing both TabHLH094–AD and TaMYC8–BD successfully grew on –Leu/–Trp/–Ade/–His dropout selection medium (Fig. 5a). To further validate whether TabHLH094 can physically interact with TaMYC8–BD, a BiFC assay was performed in tobacco epidermal cells. Pronounced YFP fluorescence was observed in cells cotransformed with both TabHLH094–nYFP and TaMYC8–cYFP (Fig. 5b). GST pulldown assays were performed on the purified

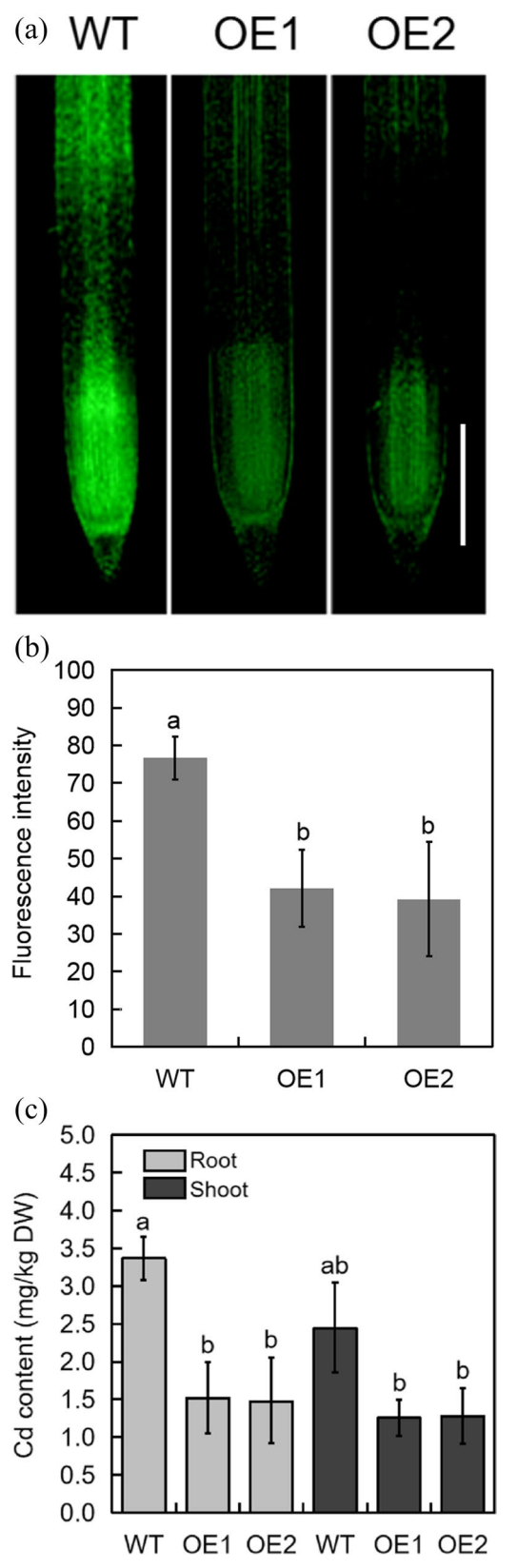

Fig. 3 Overexpression of *TabHLH094* limited Cd accumulation in root tissues. **a** Comparison of fluorescence intensities (reflective of Cd content) in the roots of WT and transgenic wheat. **b** Fluorescence intensities in root tissues were quantified using ImageJ software. The data are expressed as the means ± SDs of three independent experiments. Different lowercase letters signify significant ($P < 0.05$) differences. **c** Concentration of Cd in the roots of WT and transgenic wheat. Three-leaf-stage wheat seedlings were watered with Hoagland medium mixed with 2 mM (experimental) $CdCl_2$ for 5 days. Each value is the mean ± SE ($n = 3$). Different lowercase letters signify significant ($P < 0.05$) differences

recombinant TaMYC8–GST and TabHLH094–HIS proteins, and the results revealed that TaMYC8–GST could pull down TabHLH094–HIS (Fig. 5c). Finally, a Co–IP experiment was carried out utilizing tobacco leaves transiently expressing either TaMYC8–MYC with Flag or TabHLH094–Flag. We found that TaMYC8–MYC could be coimmunoprecipitated only with the TabHLH094–Flag fusion protein (Fig. 5d). Our results indicate that TabHLH094 can physically interact with TaMYC8 in vitro and in vivo.

A TabHLH094–TaMYC8 binary complex blocks the transcriptional activity of TaMYC8

Our previous study found that *TaMYC8* regulated the expression of *TaERF6*, thereby altering the Cd exposure response of wheat (Wang et al. 2022a, b). Here, we evaluated whether the TabHLH094–TaMYC8 binary complex affects the ability of TaMYC8 to bind to the *TaERF6* promoter. EMSA indicated that the band signal of the TaMYC8–HIS protein and *TaERF6* promoter complex was significantly reduced after the addition of the TabHLH094–HIS protein (Fig. 6a). LCI assays in tobacco leaves revealed a strong luminescence signal localized to the TaMYC8 and TaERF6 promoter coinjection area, with minimal signals observed in the TabHLH094, TaMYC8, and TaERF6 promoter coinjection areas (Fig. 6b). Together, these results indicate that the TabHLH094–TaMYC8 binary complex inhibits the ability of TaMYC8 to bind to the promoter of TaERF6 both in vivo and in vitro.

Overexpression of *TabHLH094* inhibits the activities of ACS and ACO

The *ERF* gene encodes a TF that regulates ethylene synthesis, and both ACO and ACS are rate-limiting

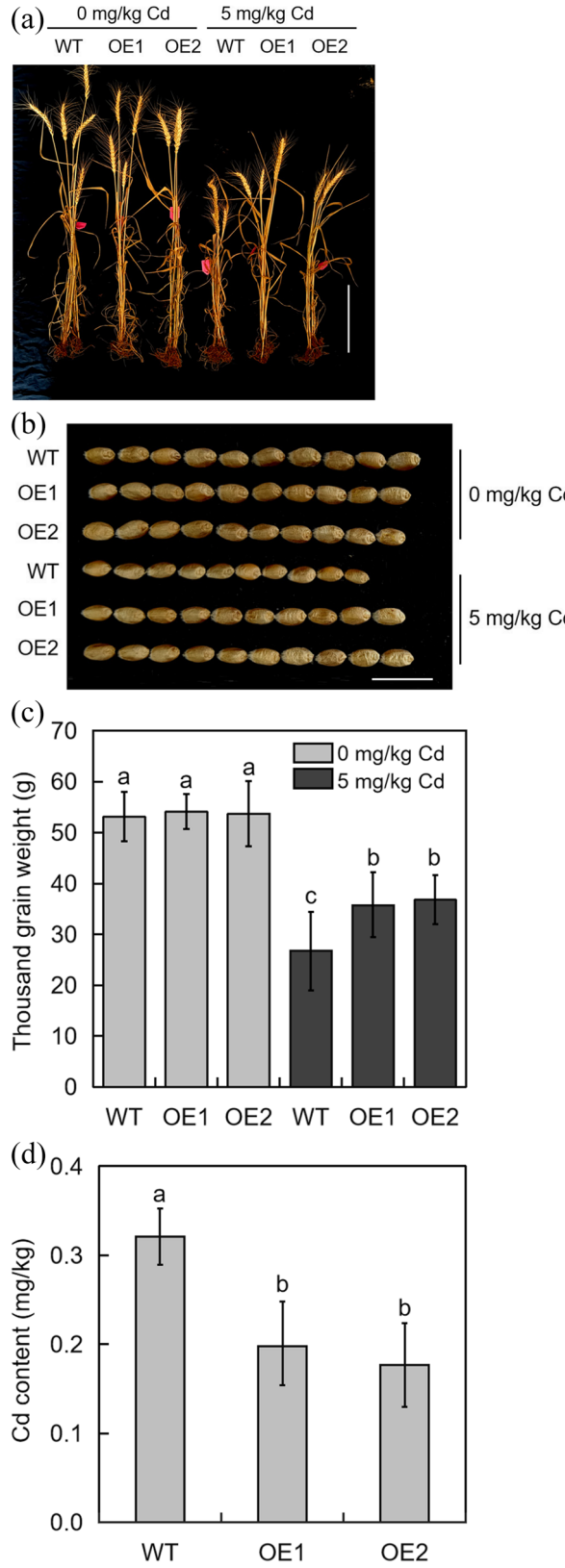

Fig. 4 **a** Plant phenotypes of WT and *TabHLH094* overexpression lines were observed with or without Cd. Scale = 30 cm. **b** Grain phenotypes of WT and *TabHLH094* overexpression lines were observed with or without Cd. Scale = 2 cm. **c** Thousand-grain weight of WT and *TabHLH094* overexpression lines under control and Cd stress conditions. Each value is the mean ± SE ($n = 3$). Different lowercase letters signify significant ($P < 0.05$) differences. **d** Cd content in the grains of WT and *TabHLH094* overexpression lines under 5 mg/kg Cd conditions. Each value is the mean ± SE ($n = 3$). Different lowercase letters signify significant ($P < 0.05$) differences

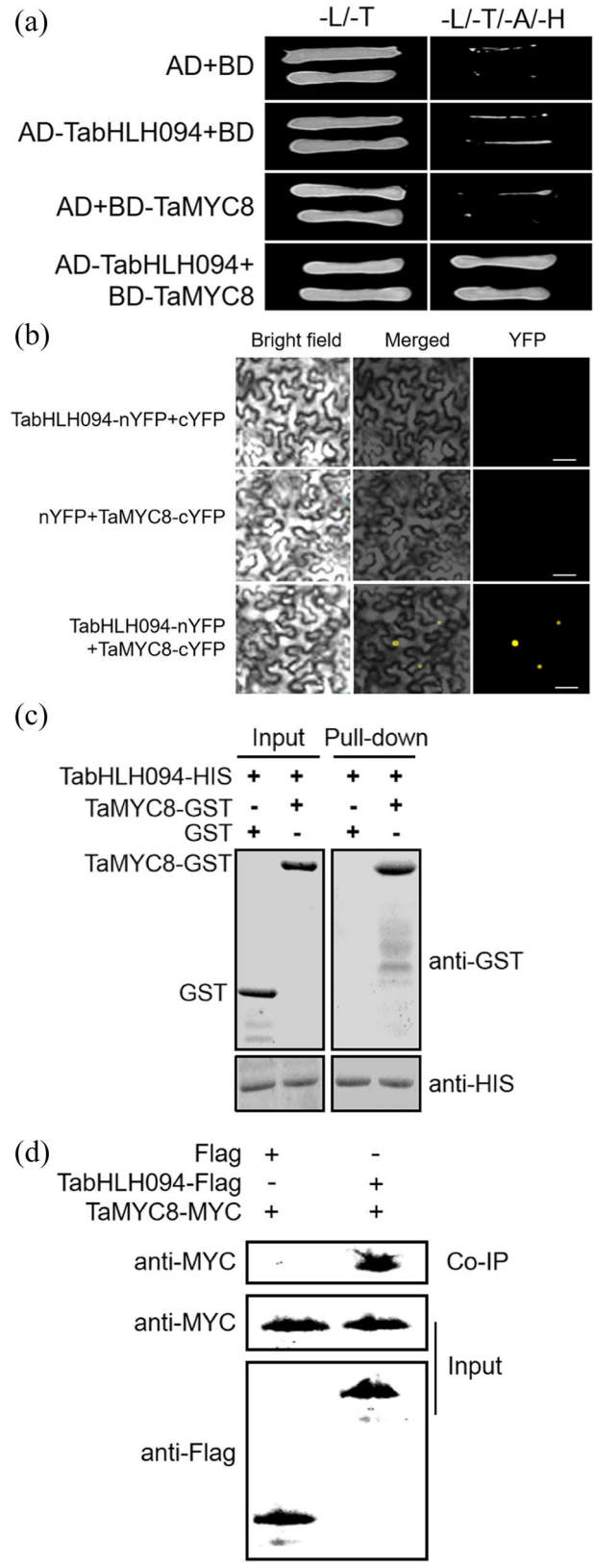

Fig. 5 TabHLH094 interacts with TaMYC8 to improve tolerance to Cd exposure. **a** Y2H analysis of the TabHLH094–TaMYC8 interaction. L: leucine, T: tryptophan, A: alanine, H: histidine. **b** BiFC analysis of TabHLH094–nYFP and TaMYC8–cYFP in tobacco leaf cells. Scale bars = 30 μm. **c** Pulldown assays indicating that TabHLH094 physically interacts with TaMYC8 in vitro. **d** Co–IP assays indicating that TabHLH094 physically interacts with TaMYC8 in vivo

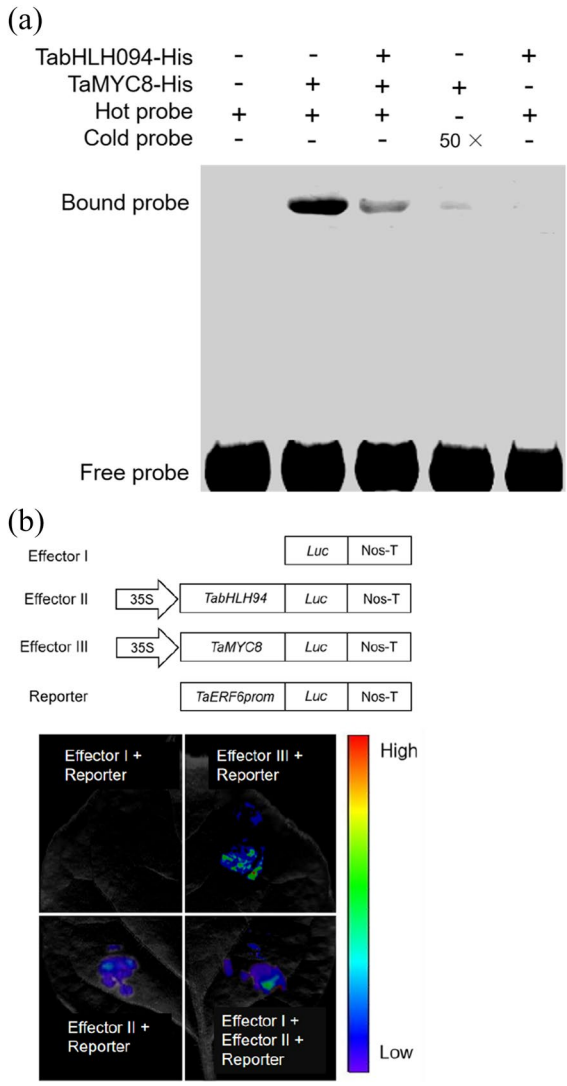

Fig. 6 The TabHLH094–TaMYC8 binary complex blocks the transcriptional activation activity of TaMYC8. **a** In vitro EMSA indicating that the band signal of the TaMYC8-*TaERF6* promoter was significantly reduced after the addition of the TabHLH094–HIS protein. **b** LCI assays indicating that the TabHLH094–TaMYC8 binary complex blocks the transcriptional activity of TaMYC8

enzymes involved in ethylene synthesis (Yin et al. 2018). Because our results indicated that the TabHLH094–TaMYC8 binary complex inhibits the ability of TaMYC8 to bind to the promoter of *TaERF6* and thereby inhibits *TaERF6* expression (Fig. 6a, b), we sought to determine whether the enzymatic activities of ACO and ACS were correspondingly inhibited in *TabHLH094*-overexpressing wheat lines. Under Cd stress, *TabHLH094*-overexpressing wheat lines exhibited significantly lower ACS and ACO activities than WT plants (Fig. 7a, b). Therefore, it appears that the overexpression of *TabHLH094* can inhibit the enzymatic activity of ACO and ACS, thereby reducing ethylene biosynthesis and improving Cd stress tolerance.

Discussion

The excessive accumulation of the phytohormone ethylene promotes maturation and reduces tolerance to heavy metal exposure (An et al. 2017). Our previous study revealed that *TaMYC8* negatively regulates tolerance to Cd exposure in wheat (Wang et al. 2022a, b). Furthermore, we revealed that Cd exposure promoted the expression of *TaEFR6*, an ethylene-responsive TF, as well as the activities of ACO and ACS (Wang et al. 2022a, b). Here, we discovered that TabHLH094 directly interacts with TaMYC8 to form a binary complex that inhibits the ability of TaMYC8 to transcriptionally regulate *TaERF6*, thereby conferring enhanced tolerance to Cd exposure.

The primary route of Cd exposure in humans is the ingestion of crops produced on Cd-polluted soils (Luo et al. 2012). Therefore, reducing the Cd content of crop plants may be an effective way to limit the exposure of animals and humans to toxic levels of Cd. Several genes have been discovered to decrease the accumulation of Cd in plant tissues. For example, several ERF TFs, including *ERF34* and *ERF35*, have been reported to be central to the Cd exposure response in plants (Xie et al. 2021). In soybean, *GmWRKY142* limits the accumulation of Cd by upregulating the *Cd tolerance type 1* genes *GmCDT1–2* and *GmCDT1–1* (Cai et al. 2020). The purpose of creating a Cd-tolerant wheat line is not only to promote plant growth under Cd stress conditions but also to minimize Cd accumulation in the edible parts. Here, we found that *TabHLH094* overexpression enhanced the growth and development of wheat under Cd conditions (Fig. 2a and Fig. 4a–c). Furthermore, in both seedlings and grains, *TabHLH094* overexpression lines accumulated significantly less Cd than WT plants (Fig. 3 and 4d).

The plant response to abiotic stress involves an array of TFs, particularly bHLH TFs (Dong et al. 2021), which regulate the abiotic stress response in two ways.

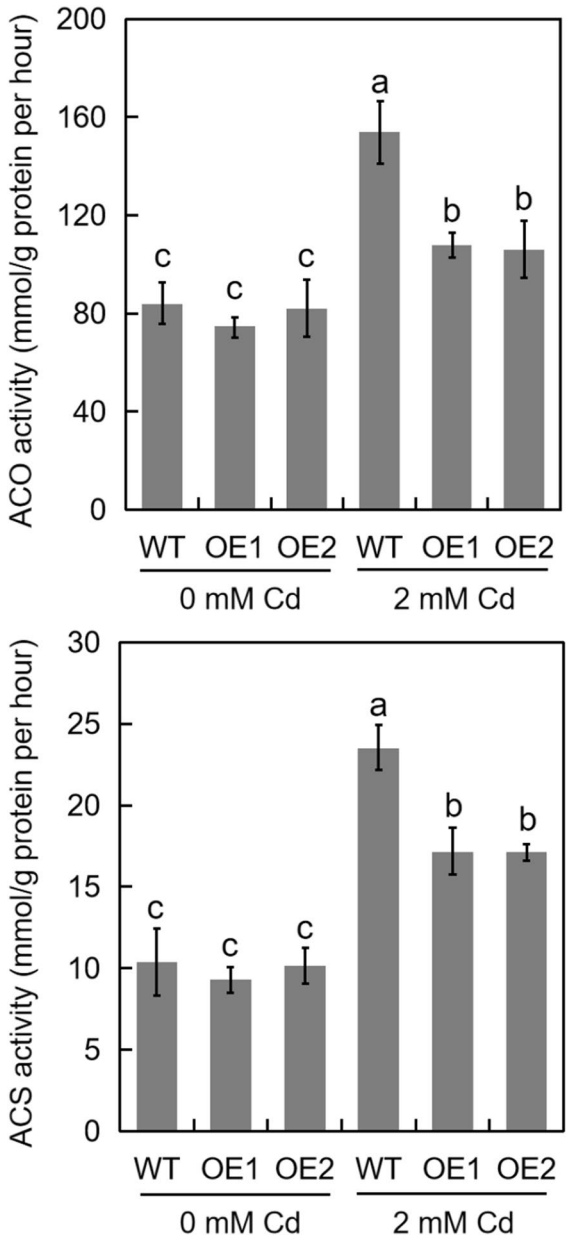

Fig. 7 The effect of Cd exposure on the activities of (**a**) ACO and (**b**) ACS in TabHLH094-overexpressing wheat. Three-leaf-stage wheat seedlings were watered with Hoagland medium mixed with 2 mM (experimental) $CdCl_2$ for 5 days. Each value is the mean ± SE ($n = 3$). Different lowercase letters signify significant ($P < 0.05$) differences

First, bHLH TFs can directly modulate downstream gene expression. For example, in apple, the bHLH-type TF *MdMYC2* curtails tolerance to aluminum (Al) exposure through direct regulation of *MdERF3* expression (An et al. 2017). Our previous study revealed that the bHLH-type TF TaMYC8 regulates TaERF6 expression, thereby weakening the Cd exposure tolerance of wheat plants (Wang et al. 2022a, b). Second, bHLH TFs can form complexes with other TFs to modulate downstream gene expression. In *Phalaenopsis*, anthocyanin biosynthesis is regulated by a MYB–bHLH complex involving PeMYC4 and PeMYB4L (Wang et al. 2022a, b). In *Eriobotrya japonica*, the EjbHLH1–EjMYB2–EjAP2–1 ternary complex acts to delay cold-induced lignification (Xu et al. 2019). The IbPYL8–IbbHLH66–IbbHLH118 ternary complex in sweet potato regulates the drought stress response by mediating the expression of *tonoplast intrinsic protein 1* (*IbTIP1*), *ABA-responsive element-binding factor 2* (*IbABF2*), and *ABA-insensitive 5* (*IbABI5*) (Xue et al. 2022). In this study, *TabHLH094* enhanced Cd tolerance in wheat by forming a binary complex with *TaMYC8* and repressing the expression of the downstream *TaERF6* gene (Figs. 5 and 6).

Several phytohormones act to regulate the plant response to stress as well as other physiological functions (Wu et al. 2020). In particular, the phytohormone ethylene negatively regulates the reaction of plants to exposure to Cd (Schellingen et al. 2014). In *Petunia hybrida*, *acdS* overexpression limits ethylene biosynthesis in both floral and vegetative tissues, thereby enhancing the lifespan of the flowers and the tolerance to Cd stress (Naing et al. 2022). The process of Cd-induced ethylene production relies on *ACO* and *ACS* gene expression (Schellingen et al. 2014). Reducing *ACS* and *ACO* gene expression, which results in reduced ethylene biosynthesis, can improve plant tolerance to environmental stress (Li et al. 2019; Espley et al. 2019). Here, we found that the overexpression of *TabHLH094* resulted in reduced ACO and ACS activities (Fig. 7), which would likely result in reduced ethylene biosynthesis.

Conclusion

Here, we report the identification of the bHLH-type TF *TabHLH094*, which positively regulates Cd stress tolerance in wheat. TabHLH094 can interact with TaMYC8, inhibit the ability of TaMYC8 to bind to the promoter of *TaERF6*, and downregulate *TaERF6* expression. These actions should result in a reduction in ethylene biosynthesis, further improving Cd stress

tolerance in wheat. The results of this study help clarify the mechanism by which the bHLH TF *TabHLH094* regulates the wheat Cd stress response. This TF may prove to be a fruitful target for the breeding of wheat with reduced Cd accumulation.

Funding This work was supported by the Precursor Projects of Guizhou Province for Biological Breeding Supporting by Science and Technology in 2022 (QKHZC2022ZD026), National Natural Science Foundation of China (grant no. 32260506), and the Science and Technology Department of Guizhou Province, China (grant no. ZK2022YB315).

Data availability All data generated during the study are given in this published article.

References

An JP, Wang XN, Yao JF, Ren YR, You CX, Wang XF, Hao YJ (2017) Apple *MdMYC2* reduces aluminum stress tolerance by directly regulating *MdERF3* gene. Plant Soil 418:255–266

Brunetti P, Zanella L, De Paolis A, Di Litta D, Cecchetti V, Falasca G, Barbieri M, Altamura MM, Costantino P, Cardarelli M (2015) Cadmium–inducible expression of the ABC–type transporter AtABCC3 increases phytochelatin–mediated cadmium tolerance in *Arabidopsis*. J Exp Bot 66:3815–3829

Chen HC, Cheng WH, Hong CY, Chang YS, Chang MC (2018) The transcription factor *OsbHLH035* mediates seed germination and enables seedling recovery from salt stress through ABA–dependent and ABA–independent pathways, respectively. Rice 11:50

Cai Z, Xian P, Wang H, Lin R, Lian T, Cheng Y, Ma Q, Nian H (2020) Transcription factor *GmWRKY142* confers cadmium resistance by up–regulating the *Cadmium Tolerance 1–Like* genes. Front Plant Sci 11:724

Dong H, Chen Q, Dai Y, Hu W, Zhang S, Huang X (2021) Genome–wide identification of *PbrbHLH* family genes, and expression analysis in response to drought and cold stresses in pear (*Pyrus bretschneideri*). BMC Plant Biol 21:86

Elobeid M, Göbel C, Feussner I, Polle A (2012) Cadmium interferes with auxin physiology and lignification in poplar. J Exp Bot 63:1413–1421

Espley RV, Leif D, Plunkett B, McGhie T, Henry-Kirk R, Hall M, Johnston JW, Punter MP, Boldingh H, Nardozza S, Volz RK, O'Donnell S, Allan AC (2019) Red to brown: an elevated anthocyanic response in apple drives ethylene to advance maturity and fruit flesh browning. Front Plant Sci 10:1248

Jin P, Chao K, Li J, Wang Z, Cheng P, Li Q, Wang B (2021) Functional verification of two genes related to stripe rust resistance in the wheat–*Leymus mollis* introgression line M8664–3. Front Plant Sci 12:754823

Luo BF, Du ST, Lu KX, Liu WJ, Lin XY, Jin CW (2012) Iron uptake system mediates nitrate–facilitated cadmium accumulation in tomato (*Solanum lycopersicum*) plants. J Exp Bot 63:3127–3136

Liu F, Li XX, Wang MR, Wen J, Yi B, Shen JX, Ma CZ, Fu TD, Tu JX (2018) Interactions of WRKY15 and WRKY33 transcription factors and their roles in the resistance of oilseed rape to *Sclerotinia* infection. Plant Biotech J 16:911–925

Li X, Feng H, Wen J, Dong J, Wang T (2018) MtCAS31 aids symbiotic nitrogen fixation by protecting the leghemoglobin MtLb120–1 under drought stress in *Medicago truncatula*. Front Plant Sci 9:633

Li G, Zhang L, Wang M, Di D, Kronzucker HJ, Shi W (2019) The *Arabidopsis AMOT1/EIN3* gene plays an important role in the amelioration of ammonium toxicity. J Exp Bot 70:1375–1388

Leškovï A, Zvarï KM, Araya T, Giehl RFH (2020) Nickel toxicity targets cell wall–related processes and PIN2–mediated auxin transport to inhibit root elongation and gravitropic responses in *Arabidopsis*. Plant Cell Physiol 61:519–535

Mao K, Dong Q, Li C, Liu C, Ma F (2017) Genome wide identification and characterization of apple bHLH transcription factors and expression analysis in response to drought and salt stress. Front Plant Sci 8:480

Ma QJ, Sun MH, Lu J, Hu DG, Kang H, You CX, Hao YJ (2020a) Phosphorylation of a malate transporter promotes malate excretion and reduces cadmium uptake in apple. J Exp Bot 71:3437–3449

Ma H, Wei M, Wang Z, Hou S, Li X, Xu H (2020) Bioremediation of cadmium polluted soil using a novel cadmium immobilizing plant growth promotion strain *Bacillus* sp. TZ5 loaded on biochar. J Hazard Mater 388:122065

Naing AH, Campol JR, Chung MY, Kim CK (2022) Overexpression of *acdS* in *Petunia hybrida* improved flower longevity and cadmium–stress tolerance by reducing ethylene production in floral and vegetative tissues. Cells 11:3197

Qi T, Song S, Ren Q, Wu bD, Huang H, Chen Y, Fan M, Peng W, Ren C (2011) Xie D (2011) The Jasmonate–ZIM–domain proteins interact with the WD–Repeat/bHLH/MYB complexes to regulate Jasmonate–mediated anthocyanin accumulation and trichome initiation in *Arabidopsis thaliana*. Plant Cell 23:1795–814

Schellingen K, Van Der Straeten D, Vandenbussche F, Vandenbussche F, Prinsen E, Remans T, Vangronsveld J, Cuypers A (2014) Cadmium–induced ethylene production and responses in *Arabidopsis thaliana* rely on *ACS2* and *ACS6* gene expression. BMC Plant Biol 14:214

Song YS, Yang WJ, Fan H, Zhang XS, Sui N (2020) TaMYB86B encodes a R2R3–type MYB transcription factor and enhances salt tolerance in wheat. Plant Sci 300:110624

Wu H, Chen C, Du J, Liu H, Cui Y, Zhang Y, He Y, Wang Y, Chu C, Feng Z, Li J, Ling HQ (2012) Co–overexpression FIT with AtbHLH38 or AtbHLH39 in *Arabidopsis*–enhanced cadmium tolerance via increased cadmium sequestration in roots and improved iron homeostasis of shoots. Plant Physiol 158:790–800

Wu L, Li J, Li Z, Zhang F, Tan X (2020) Transcriptomic analyses of *Camellia oleifera* 'Huaxin' leaf reveal candidate genes related to long–term cold stress. Int J Mol Sci 21:846

Wei S, Xia R, Chen C, Shang X, Ge F, Wei H, Chen H, Wu Y, Xie Q (2021) *ZmbHLH124* identified in maize recombinant inbred lines contributes to drought tolerance in crops. Plant Biotechnol J 19:2069–2081

Wang HC, Zuo D, Zhu B, Du XY, Gu L (2022a) TaMYC8 regulates TaERF6 and inhibits ethylene synthesis to confer Cd tolerance in wheat. Environ Exp Bot 198:104854

Wang R, Mao CJ, Ming F (2022b) PeMYB4L interacts with PeMYC4 to regulate anthocyanin biosynthesis in *Phalaenopsis* orchid. Plant Sci 324:111423

Xu Z, Liu X, He X, Xu L, Huang Y, Shao H, Zhang D, Tang B, Ma H (2017) The soybean basic helix–loop–helix transcription factor *ORG3–like* enhances cadmium tolerance via increased iron and reduced cadmium uptake and transport from roots to shoots. Front Plant Sci 8:1098

Xu M, Li SJ, Liu XF, Yin XR, Grierson D, Chen KS (2019) Ternary complex EjbHLH1–EjMYB2–EjAP2–1 retards low temperature–induced flesh lignification in loquat fruit. Plant Physiol Bioch 139:731–737

Xie Q, Yu Q, Jobe TO, Pham A, Ge C, Guo Q, Liu J, Liu H, Zhang H, Zhao Y, Xue S, Hauser F, Schroeder JI (2021) An amiRNA screen uncovers redundant *CBF* and *ERF34/35* transcription factors that differentially regulate arsenite and cadmium responses. Plant Cell Environ 44:1692–1706

Xue LY, Wei ZW, Zhai H, Xing SH, Wang YX, He SZ, Gao SP, Zhao N, Zhang H, Liu QC (2022) The IbPYL8–IbbHLH66–IbbHLH118 complex mediates the abscisic acid–dependent drought response in sweet potato. New Phytol 236:2151–2171

Yin W, Yu X, Chen G, Tang B, Wang Y, Liao C, Zhang Y, Hu Z (2018) Suppression of *SlMBP15* inhibits plant vegetative growth and delays fruit ripening in tomato. Front Plant Sci 9:938

Zhao Z, Zhang H, Fu Z, Chen H, Lin Y, Yan P, Li W, Xie H, Guo Z, Zhang X, Tang J (2018) Genetic–based dissection of arsenic accumulation in maize using a genome–wide association analysis method. Plant Biotechnol J 16:1085–1093

Zhang AD, Wang WQ, Tong Y, Li MJ, Grierson D, Ferguson I, Chen KS, Yin XR (2018) Transcriptome analysis identifies a zinc finger protein regulating starch degradation in kiwifruit. Plant Physiol 178:850–863